Membrane Water Treatment, *Vol. 7, No. 4 (2016) 297-311*
DOI: http://dx.doi.org/10.12989/mwt.2016.7.4.297

Mathematical modeling of humidification process by means of hollow fiber membrane contactor

Azam Marjani *[1], Ali Baghdadi [1] and Mehdi Ghadiri [2]

[1] Department of Chemistry, Arak Branch, Islamic Azad University, Arak, Iran
[2] Young Researchers and Elite Club, South Tehran Branch, Islamic Azad University, Tehran, Iran

(*Received January 13, 2016, Revised March 10, 2016, Accepted March 29, 2016*)

Abstract. Modeling and simulation of air humidification by hollow fiber membrane contactors are investigated in the current study. A computational fluid dynamic model was developed by solving the k-epsilon turbulence 2D Navier–Stokes equations as well as mass conservation equations for steady-state conditions in membrane contactors. Finite element method is used for the study of the air humidification under different operating conditions, with a focus on the humidity density, total mass transfer flux and velocity field. There has been good agreement between simulation results and experimental data obtained from literature. It is found that the enhancement of air stream decreases the outlet humidity from 0.392 to 0.340 (module 1) and from 0.467 to 0.337 (module 2). The results also indicated that there has been an increase in air velocity in the narrow space of shell side compared with air velocity wide space of shell side. Also, irregular arrangement has lower dead zones than regular arrangement which leads to higher water flux.

Keywords: membrane processes; simulation; mass transfer; humidification; cross flow

1. Introduction

Control of the air humidity in the transportation vehicles, buildings, ventilating and air-conditioning systems is very vital (Kneifel *et al*. 2006). In winter season relative humidity become less than standard limit (60% RH) namely 20-40% RH when an area gets warm. In such condition people feel dryness and as a result they suffer from great discomfort. However, air humidity should be existed with warm air in winter (Huang and Yang 2014, Kong *et al*. 2015, Zhang and Huang 2011). Humidification of gas stream plays important role in the industrial processes and home usage such as sweeting of natural gas (Li and Ito 2008). It is because the existence of water in natural gas causes pipe corrosion and solid methane hydrate blocking pipe lines (Wu *et al*. 2002). Mechanical dehumidifier that condenses the water vapor in the air using decreasing temperature is applied in the dehumidification process from air. However, the dry air in the room is humidified via direct atomization (Li and Ito 2008). There are different techniques to provide humidity including spray tower, ultrasonic adding humidity and steam generator. Each of these systems has their benefits and drawbacks. For instance, adding humidity using steam generator has great advantage including low cost and cleanness while it has some limitation such as high consumption

*Corresponding author, Ph.D., E-mail: a-marjani@iau-arak.ac.ir

http://www.techno-press.org/?journal=mwt&subpage=7 ISSN: 2005-8624 (Print), 2092-7037 (Online)

of energy for producing steam and direct contact between air stream and liquid which cause growing micro-organism in the air (Zhang and Huang 2011). Membrane separation technique was used in many industrial processes (Barati *et al*. 2014, Daraei *et al*. 2014, Ghadiri *et al*. 2014a, Roostaiy Ghalehnooiy *et al*. 2015). This technique can be used for separation of water from air stream, adding water to air and solved aforementioned issues regarding humidification and dehumidification (Bergero and Chiari 2001, 2010 Kong *et al*. 2015, Li and Ito 2008). Only water is able to permeate through pores of membrane (Huang *et al*. 2013).

There have been several investigations on humidification process. Yonglie *et al*. (Wu *et al*. 2002) studied dehumidification processes of compressed air in integrated membranes. To control air humidity in hollow fiber membrane contactor Keifel *et al*. (2006) studied influence of several operational parameters on this system. Li *et al*. (Li and Ito 2008) used a wet membrane system to add humidity and dehumidification from air. Triethylene glycol (TEG) was used on the surface to modify surface of hydrophobic microporous membrane. Composite membrane including poly(2-dimethylaminoethyl methacrylate) (PDMAEMA) as active layer and poly acrylo nitrile (PAN) as bed were used for transferring water vapor (Du *et al*. 2010). Chao *et al*. (Chao and Jen 2013) considered a new method to control humidity and heat of cathodic air for a fuel cell stack by utilizing indirect laser absorption spectrometry and provide a heat and humidity control strategy.

In the recent years adding humidity to air was not paid attention compared to dehumidification. It should be noted that the adding humidity to air is very important in HVAC industries (Zhang 2012). In addition, modeling and simulation of this process is very important, while, there are little published literatures in this regard. Mathematical modelling and simulation of different processes including gas absorption, gas stripping and non-disperse extraction via hollow fiber membrane contactor have been studied by some researcher (Ghadiri *et al*. 2013c, 2014c, 2015, Ghadiri and Ashrafizadeh 2014, Shirazian *et al*. 2012a, Tahvildari *et al*. 2014). The hollow fiber membrane module for adding humidity to air is considered for investigation in this work. This module operates same as a shell and tube heat exchanger (Zhang and Li 2013).

The current study presents a new procedure for modeling and simulation of simultaneous momentum and mass transfer in hollow fiber membrane contactor for inline and staggered arrangements. A standard k-epsilon turbulence model and continuity equations are applied to predict velocity fields and concentration distribution of air humidification system. Then the numerical model is validated by experimental data. Various parameters including distribution of water concentration in HFMC, Total flux of mass transfer and velocity fields are studied for both arrangements.

2. Theory

A 2D mathematical model was proposed for transport of water through hollow fiber membrane contactor with cross flow. Set of hollow fiber membranes are inside the pipe and there is space between external shell and fibers inside the shell. Water and air enter in membrane contactor in cross-flow arrangement (Huang and Yang 2014, Huang *et al*. 2013). Water flows from tube side whereas air passes from shell side of membrane contactor. Fig. 1 illustrates the geometric models of the hollow fiber membrane contactor which is considered in the present work (Zhang and Li 2013).

The air stream flows in the shell side with cross flow, whereas the pure water is fed to the tube side of the HFMC. The air stream velocity field in the shell side was determined using Navier–Stokes equations. Axial and radial diffusions through the membrane and within the shell side of

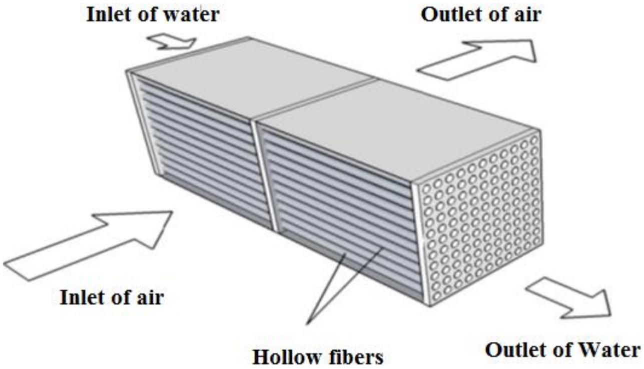

Fig. 1 Schematic diagram of cross-flow hollow fiber membrane module for air humidification (Zhang and Li 2013)

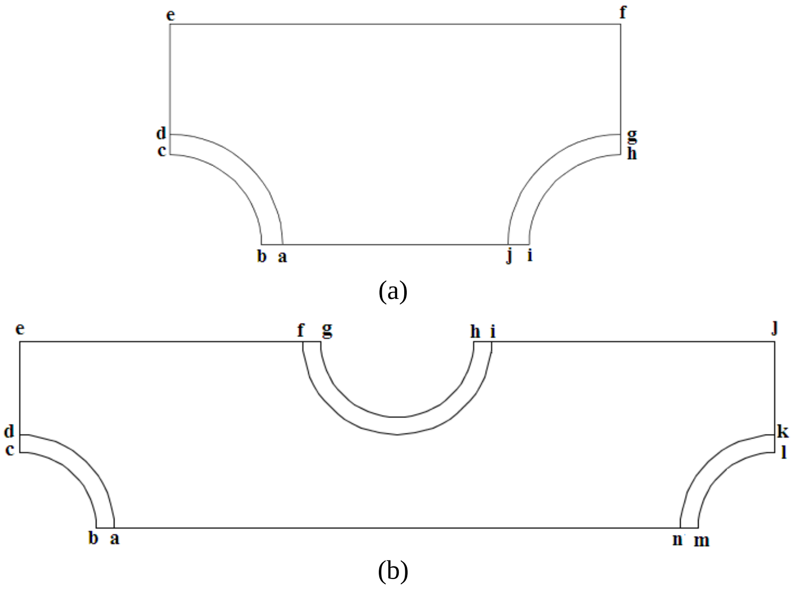

Fig. 2 Computational domains: (a) fibers with regular arrangements; (b) fibers with irregular arrangements

HFMC are considered in the model equations. Pure water permeates through fibers and diffuses in to the shell side, so it leads to the enhancement of air stream humidity. For simulation of humidification process a simple shape are considered. The HFMC consists of two sections: membrane, and shell side. The fibre membranes are made with a modified PVDF material.The steady state 2D mass balances are carried out for all two sections of the HFMC.

The model is built considering the following assumptions:

(1) Steady state and physical condition is constant.
(2) The force of gravity is ignored.
(3) Air-flow has developed before entering in system.
(4) Establishing the mass affinity law in membranes and shell interface for humidity.

Table 1 Physical properties and geometrical parameters of module used in the simulation (Zhang and Li 2013)

Name of properties	Symbol	Unit	Module 1	Module 2
Array arrangement			In-line	Staggered
Effective fiber length	L	mm	350	380
Number of fibers in the module	n		1860	4100
Fiber outer diameter	d	mm	1.6	1.6
Membrane thickness	δ	mm	0.15	0.15
Membrane porosity	ε	-	0.75	0.75
Moisture diffusivity in air	$D_{H2O,\ S}$	$m^2.s^{-1}$	2.82e-5	2.82e-5
Effective diffusivity in membrane	$D_{H2O,\ m}$	$m^2.s^{-1}$	1.33e-6	1.33e-6
Air flow rate (inline)	$U\infty$	$m.s^{-1}$	0.91-2.72	0.92-2.82
Air inlet temperature	T_{inlet}	K	299.3	298.9

Schematic of the model domain used in simulation of In-line and staggered contactors in 2D is shown in Fig. 2. Also, Table 1 presents physical and geometrical parameters for the In-line and staggered models.

2.1 Model equations

Mass and momentum transfer equations are written and solved numerically to estimate concentration and velocity distributions in the membrane contactor.

2.1.1 Membrane side equations

The steady-state continuity equation for transport of water inside the membrane, which is considered to be due to diffusion alone, may be written as (Bird *et al*. 2002, Ghadiri *et al*. 2013a, b, 2014b)

$$\nabla.(-D_{H_2O,m}\nabla C_{H_2O,m}) = R_i \tag{1}$$

where $C_{H2O,m}$ is the water concentration (mol.m^{-3}). $D_{H2O,m}$ and R_i denote diffusion coefficient of water and the reaction term respectively. It should be pointed out that chemical reaction does not occur in the model domain, so it is omitted in the continuity equation in the simulation. Boundary conditions for membrane with regular and irregular arrangements are shown in Table 2. Positions can be found in Fig. 2 for regular (a) and irregular (b) arrangements.

2.1.2 Shell side equations

The steady state continuity equation without chemical reaction for water in the shell side of the HFMC in cylindrical coordinate is obtained using Fick’s law of diffusion for estimation of diffusive and convective fluxes (Bird *et al*. 2002, Ghadiri and Shirazian 2013, Ghadiri *et al*. 2012)

$$\nabla.(-D_{H_2O,s}\nabla C_{H_2O,s}) = -U_{H_2O,s}.\nabla C_{H_2O,s} \tag{2}$$

where $C_{H2O,s}$ is the water concentration (mol.m^{-3}), $D_{H2O,s}$ (m^2.s^{-1}) and $U_{H2O,s}$ (m.s^{-1}) are the diffusion coefficient and the water velocity in the shell side of hollow fiber membrane contactor. This

Table 2 Boundary conditions of membrane side equations for (a) regular; and (b) irregular arrangements

Position	Regular arrangement	Irregular arrangement
cb	C_{H2O} @ P^{sat} = 0.959	C_{H2O} @ P^{sat} = 0.959
hk	C_{H2O} @ P^{sat} = 0.959	
ad	$C_{H2O,m} = C_{H2O,s}$	
gl	$C_{H2O,m} = C_{H2O,s}$	
cd	Insulation/symmetry	Insulation/symmetry
ab	Insulation/symmetry	Insulation/symmetry
lk	Insulation/symmetry	Insulation/symmetry
gh	Insulation/symmetry	
kg	-	C_{H2O} @ P^{sat} = 0.959
op	-	C_{H2O} @ P^{sat} = 0.959
ad	-	$C_{H2O,m} = C_{H2O,s}$
fl	-	$C_{H2O,m} = C_{H2O,s}$
nq	-	$C_{H2O,m} = C_{H2O,s}$
fg	-	Insulation/symmetry
no	-	Insulation/symmetry
pq	-	Insulation/symmetry

equation should be solved numerically to obtain the water ($C_{H2O,s}$) concentration distribution in the hollow fiber membrane contactor. However, to solve the continuity equation, (Eq (2)), the velocity distribution ($U_{H2O,s}$) is required (Miramini *et al*. 2013, Nosratinia *et al*. 2014).

Velocity distribution in the shell side can be determined by solving the momentum equation such as Navier–Stokes equations. So, the momentum and the continuity equations should be coupled and solved simultaneously to obtain the water concentration distribution in the shell side of the contactor. The Navier–Stokes equations describe flow in viscous fluids through momentum balances for water. They also assume that viscosity and density of the water vapors are constant, which yields to a continuity condition.A standard k-epsilon turbulence model, which has been proved to predict the velocity fields better than other turbulence models for fiber bundles was used in the current study (Paul *et al*. 2008). The Navier–Stokes equations (k-3) in the turbulent condition are defined as follows (Bird *et al*. 2002)

$$\rho(\mathrm{U}_{\mathrm{H_2O,s}}.\nabla)\mathrm{U}_{\mathrm{H_2O,s}} = \nabla.[-PI + (\eta+\eta_T)(\nabla\mathrm{U}_{\mathrm{H_2O,s}} + (\nabla\mathrm{U}_{\mathrm{H_2O,s}})^T)] + \mathrm{F} \tag{3}$$

$$\nabla.\mathrm{U}_{\mathrm{H_2O,s}} = 0 \tag{4}$$

$$\rho\mathrm{U}_{\mathrm{H_2O,s}}.\nabla K = \nabla.[(\eta+\eta_T/\sigma_K)\nabla K] + \eta_T \mathrm{p}(\mathrm{U}_{\mathrm{H_2O,s}}) - \rho\varepsilon \tag{5}$$

$$\rho\mathrm{U}_{\mathrm{H_2O,s}}.\nabla\varepsilon = \nabla.[(\eta+\eta_T/\sigma_\varepsilon)\nabla\varepsilon] + C_{\varepsilon 1}\varepsilon\eta_T \mathrm{p}(\mathrm{U}_{\mathrm{H_2O,s}})/K - C_{\varepsilon 2}\rho\varepsilon^2/K \tag{6}$$

$$\rho(\mathrm{U}_{\mathrm{H_2O,s}}) = \nabla\mathrm{U}_{\mathrm{H_2O,s}} : (\nabla\mathrm{U}_{\mathrm{H_2O,s}} + (\nabla\mathrm{U}_{\mathrm{H_2O,s}})^T), \eta_T = C_\mu \rho K^2/\varepsilon \tag{7}$$

Table 3 Boundary conditions of shell side equations for (a) regular, and (b) irregular arrangements

Position	Regular arrangement (mass transfer)	Irregular arrangement (mass transfer)	Regular arrangement (momentum)	Irregular arrangement (momentum)
de	$C_{H2O\text{-inlet}} = C_0$	$C_{H2O\text{-inlet}} = C_0$	$U_{H2O\text{-inlet}} = U_0$	$U_{H2O\text{-inlet}} = U_0$
ad	$C_{vs} = C_{vm}$	$C_{vs} = C_{vm}$	Wall	Wall
gl	$C_{vs} = C_{vm}$	-	Wall	
fg	Convective flux	-	P = 0	
al	Insulation/symmetry	Insulation/symmetry	Insulation/symmetry	
ef	Insulation/symmetry	Insulation/symmetry	Insulation/symmetry	Insulation/symmetry
fl	-	$C_{vs} = C_{vm}$	-	Wall
nq	-	$C_{vs} = C_{vm}$	-	Wall
mn	-	Convective flux	-	P = 0
lm	-	Insulation/symmetry	-	Insulation/symmetry
qa	-	Insulation/symmetry	-	Insulation/symmetry

where F, $U_{H2O,s}$, η, ρ and P denote body force term (N), velocity ($m.s^{-1}$), viscosity ($kg.m^{-1}.s^{-1}$), density ($kg.m^{-3}$) and pressure (Pa) respectively. Boundary conditions for mass transfer and momentum equations in the shell side with regular and irregular arrangements are given in Table 3. Positions can be found in Fig. 2 for (a) regular; and (b) irregular arrangements.

2.2 Numerical solution

The aforementioned model equations related to hollow fiber membrane contactors with the boundary conditions were solved using COMSOL Multiphysics software (version 3.5) (Shirazian and Ashrafizadeh 2010). This software uses finite element method (FEM) analysis for numerical solution of the developed equations in this work. The numerical solver of UMFPACK version 4.2 was applied as a direct solver which is appropriate for numerical solution of stiff and non-stiff nonlinear boundary value problems. The UMFPACK solver can always solve the transposed problem at the cost of a back-substitution, while remaining direct solvers need to do a new factorization if the problem is not symmetric or Hermitian.

A system with the specifications of RAM 4.00 GB (2.98 GB usable) and Intel® Core™ i5CPU M 480 @ 2.67 GHz and 32-bit operating system was used to solve the model equations. Adaptive mesh refinement in COMSOL, which generates the best and minimal meshes, was used to mesh the membrane contactor geometry. The accuracy, applicability, and robustness of this approach for the simulation of membrane contactors have been proved by some researchers (Ghadiri *et al*. 2014b, Ghadiri and Shirazian 2013, Hemmati *et al*. 2015, Miramini *et al*. 2013, Nosratinia *et al*. 2014).

3. Results and discussion

3.1 Model validation

The modeling results for humidification of air stream by the membrane contactor were compared with the experimental data reported by Zhang and Li (2013). The outlet concentration of

Table 4 Comparison of experimental data of outlet humidity with simulation values at different air flow rate (Zhang and Li 2013)

Type	U∞ (m/s)	Experimental data ($C_{H2O,\ Outlet}$)	Modeling values ($C_{H2O,\ Outlet}$)	Efficiency (%)
(a) Module 1	0.910	0.371	0.392	49.08
	1.360	0.342	0.369	40.30
	1.810	0.325	0.357	35.66
	2.260	0.314	0.347	31.82
	2.720	0.306	0.340	29.1
(b) Module 2	0.920	0.462	0.467	88.52
	1.370	0.414	0.436	76.11
	1.910	0.385	0.410	65.77
	2.310	0.363	0.346	39.64
	2.810	0.348	0.337	36.03

water in air stream at different air stream flow rate is chosen to compare the modeling data with the experimental values. The results are presented in Table 4. As it can be seen, the modeling predictions follow the general trend of the experimental data with deviations of smaller than approximately 10% which indicate the conformity between experiments and model predictions. Furthermore, it should be pointed out that increasing air stream flow leads to a decreasing in outlet concentration of water vapor.

The separation efficiency of water vapor (last column in Table 4) which is defined the ratio of the water transfer from the tube side to shell side to total water vapor in the initial feed phase is determined by using Eq. (8) as follows

$$\text{Humidification efficiency}(\%) = \left(\frac{C_{H_2O,Outlet} - C_{H_2O,Outlet}}{C_{H_2O,Outlet}} \right) \times 100 \tag{8}$$

where $C_{H2O,Outlet}$ and $C_{H2O,Inlet}$ are water concentration at outlet and inlet of shell side of membrane contactor. The performance of system with irregular arrangement is better than the system with regular arrangement. It confirms that the two-dimensional model developed here for humidification process based on the momentum and mass transfer is accurate in estimation of humidification operation.

3.2 Concentration distribution of water in the shell and membrane sides

Concentration distribution for humidity in both membrane and shell sides in two regular and irregular arrangements are shown in Figs. 3 and 4. The water flows from tube side of the contactor where the concentration of water is the highest (C_0), whereas the air stream flows from the other side as cross flow where the concentration of water is assumed to be low. As the water flows through the tube side, water moves towards the membrane due to the concentration difference. Finally, the complex is swept by the air stream and air stream becomes humid and leaves the contactor. Figs. 3 and 4 confirm that the water penetrates through the membrane's pores and diffuses in to the shell side of membrane contactor.

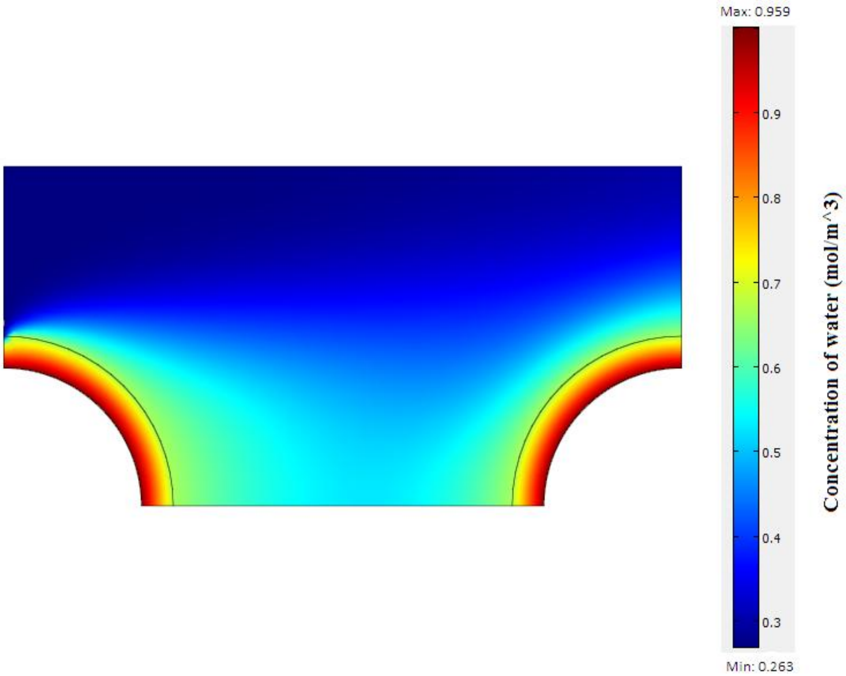

Fig. 3 Distribution of water concentration in the membrane and shell sides of contactor with regular arrangement (mol.m^{-3})

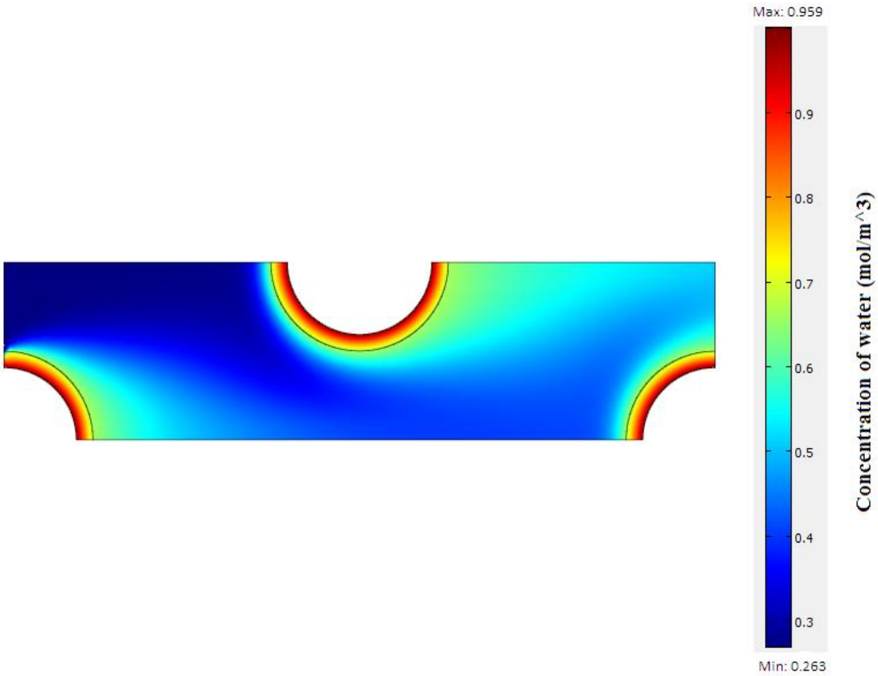

Fig. 4 Distribution of water concentration in the membrane and shell sides of contactor with irregular arrangement (mol.m^{-3})

3.3 Total mass transfer flux

Figs. 5 and 6 illustrate the total mass transfer flux of the water in the shell side of membrane contactor. The total mass flux of water vapor constitutes two mass flux including diffusion and convection mass fluxes (Fadaei *et al*. 2011, 2012, Razavi *et al*. 2013, Rezakazemi *et al*. 2013a, Shirazian *et al*. 2012b). At the outlet of shell side, the total flux is highest because the concentration distribution is highest. It is due to permeation of water in to the shell side in the outlet. As it can be also seen, contribution of convective flux in the upper segment of shell side in the *x*-direction is considerable compared to diffusive flux in this region. That is due to the fact that in the *x* direction, the velocity is considerable and results in high convective flux for water (Fadaei *et al*. 2012a, b, Shirazian and Ashrafizadeh 2011). Staggered arrangement is better for heat and mass transport in membrane contactor. It is because the staggered arrangement has lower dead zones and fluid is better mixed in the staggered arrangement than those in the in-line one (Huang *et al*. 2013).

3.4 Velocity field in the shell side of contactor

The velocity field in the shell side of the membrane contactor with two regular and irregular arrangements is illustrated in Figs. 7 and 8, where the air stream flows. The velocity field in the shell side of the contactor was simulated by solving the Navier–Stokes equations in turbulent

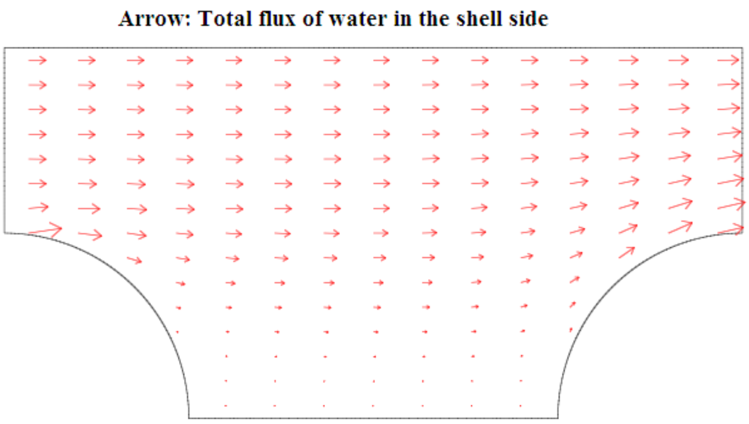

Fig. 5 Total flux of mass transfer for regular arrangement (mol.m^{-2}.s^{-1})

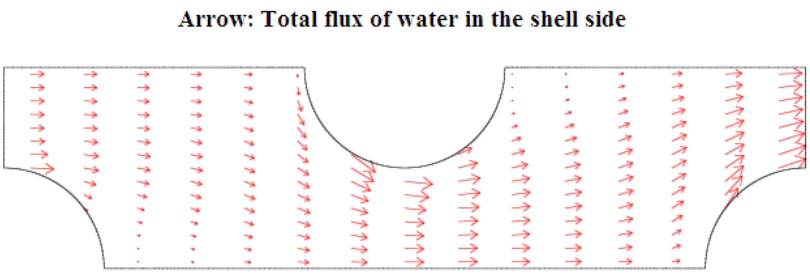

Fig. 6 Total flux of mass transfer for irregular arrangement (mol.m^{-2}.s^{-1})

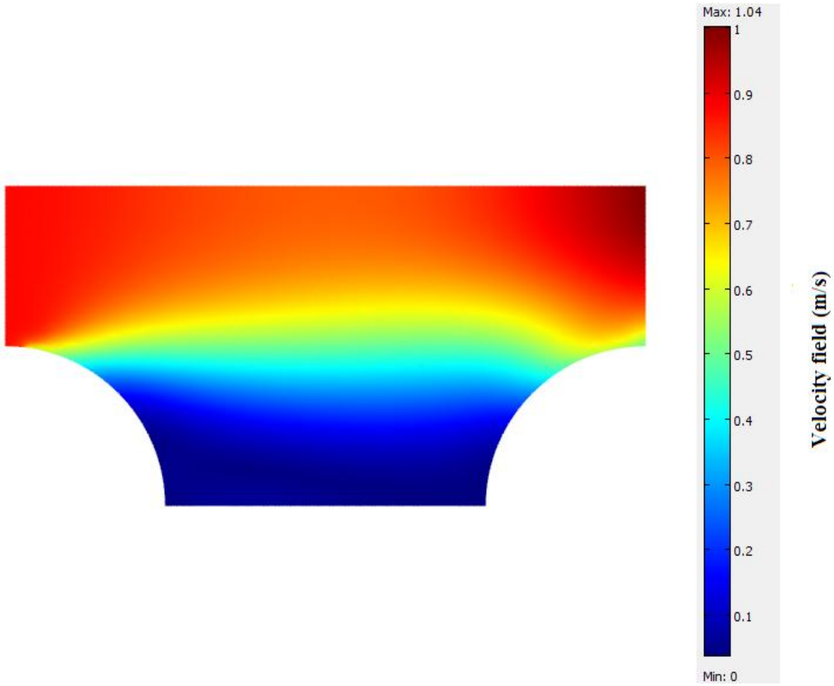

Fig. 7 Velocity field in regular arrangement (m.s^{-1})

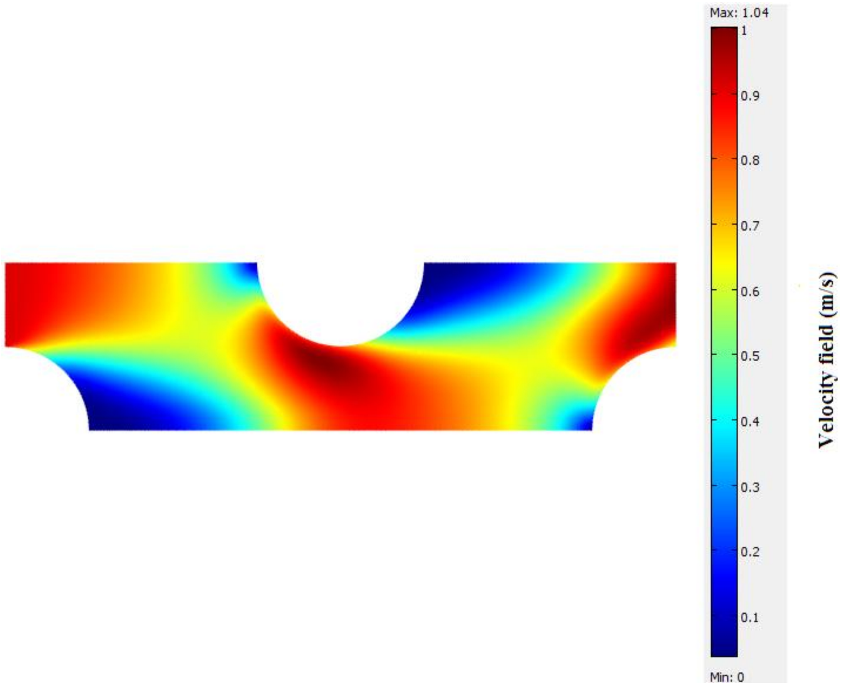

Fig. 8 Velocity field in irregular arrangement (m.s^{-1})

condition (Moradi *et al*. 2013, Rezakazemi *et al*. 2013b, Shirazian and Ashrafizadeh 2013). These results are compared with the obtained velocity fields which determined by Huang *et al*. (2013) for elliptical hollow fiber membrane contactor for in-line and staggered arrangements. The same velocity fields were obtained in both studies. Velocity is high where there is narrow space, whereas in wide spaces the velocity field is low. Fibers act as barrier against air flow which causes the enhancement of the velocity on the fibers. One of the advantages of irregular arrangement is that the dead zones are lower than regular arrangement. For this reason, the flux of water in irregular arrangement is higher than regular arrangement.

4. Conclusions

A 2D mathematical model was proposed to describe mass transfer and momentum (k-epsilon turbulence model) of adding humidity to air stream in hollow fiber membrane contactor with cross-flow. Computational fluid dynamic is used to simulate the humidification process and determine concentration and velocity distributions in membrane contactor. The simulation results for humidification of air stream indicated that the enhancement of air stream flow rate decreases the content of water vapor in the air stream in the shell side of membrane contactor. Moreover, concentration distribution near the surface of fibers is higher than upper segment of shell side which confirms the diffusion of water from tube side in to shell side through pores of membrane. There has been higher total flux for staggered arrangement with compared to inline arrangement. This is because the staggered arrangement creates more turbulent flow and has low dead zones.

References

Barati, F., Ghadiri, M., Ghasemi, R. and Nobari, H.M. (2014), "CFD simulation and modeling ofmembrane-assisted separation of organic compounds from wastewater", *Chem. Eng. Technol.*, **37**(1), 81-86.

Bergero, S. and Chiari, A. (2001), "Experimental and theoretical analysis of air humidification/humidification processes using hydrophobic capillary contactors", *Appl. Therm. Eng.*, **21**(11), 1119-1135.

Bergero, S. and Chiari, A. (2010), "Performance analysis of a liquid desiccant and membrane contactor hybrid air-conditioning system", *Energ. Buildings*, **42**(11), 1976-1986.

Bird, R.B., Stewart, W.E. and Lightfoot, E.N. (2002), *Transport Phenomena*, John Wiley & Sons, New York, NY, USA.

Chao, C.-H. and Jen, T.-C. (2013), "A new humidification and heat control method of cathode air for a PEM fuel cell stack", *Int. J. Heat Mass Tran.*, **58**(1-2), 117-124.

Daraei, A., Aghasafari, P., Ghadiri, M. and Marjani, A. (2014), "Modeling and transport analysis of silver extraction in porous membrane extractors by computational methods", *Trans. Indian Inst. Met.*, **67**(2), 223-227.

Du, J.R., Liu, L., Chakma, A. and Feng, X. (2010), "Using poly(N,N-dimethylaminoethyl methacrylate)/ polyacrylonitrile composite membranes for gas dehydration and humidification", *Chem. Eng Sci.*, **65**(16), 4672-4681.

Fadaei, F., Shirazian, S. and Ashrafizadeh, S.N. (2011), "Mass transfer modeling of ion transport through nanoporous media", *Desalination*, **281**, 325-333.

Fadaei, F., Shirazian, S. and Ashrafizadeh, S.N. (2011), "Mass transfer simulation of solvent extraction in hollow-fiber membrane contactors", *Desalination*, **275**(1-3), 126-132.

Fadaei, F., Hoshyargar, V., Shirazian, S. and Ashrafizadeh, S.N. (2012), "Mass transfer simulation of ion separation by nanofiltration considering electrical and dielectrical effects", *Desalination*, **284**, 316-323.

Fasihi, M., Shirazian, S., Marjani, A. and Rezakazemi, M. (2012), "Computational fluid dynamics

simulation of transport phenomena in ceramic membranes for SO_2 separation", *Math. Comput. Model.*, **56**(11-12), 278-286.
Ghadiri, M. and Ashrafizadeh, S.N. (2014), "Mass transfer in molybdenum extraction from aqueous solutions using nanoporous membranes", *Chem. Eng. Technol.*, **37**(4), 597-604.
Ghadiri, M. and Shirazian, S. (2013), "Computational simulation of mass transfer in extraction of alkali metals by means of nanoporous membrane extractors", *Chem. Eng. Proces: Process Intensifi.*, **69**, 57-62.
Ghadiri, M., Shirazian, S. and Ashrafizadeh, S.N. (2012), "Mass transfer simulation of gold extraction in membrane Extractors", *Chem. Eng. Technol.*, **35**(12), 2177-2182.
Ghadiri, M., Fakhri, S. and Shirazian, S. (2013a), "Modeling and CFD simulation of water desalination using nanoporous membrane contactors", *Ind. Eng. Chem. Res.*, **52**(9), 3490-3498.
Ghadiri, M., Ghasemi Darehnaei, M., Sabbaghian, S. and Shirazian, S. (2013b), "Computational simulation for transport of priority organic pollutants through nanoporous membranes", *Chem. Eng. Technol.*, **36**(3), 507-512.
Ghadiri, M., Marjani, A. and Shirazian, S. (2013c), "Mathematical modeling and simulation of CO_2 stripping from monoethanolamine solution using nano porous membrane contactors", *Int. J. Greenhouse Gas Control*, **13**, 1-8.
Ghadiri, M., Abkhiz, V., Parvini, M. and Marjani, A. (2014a), "Simulation of membrane distillation for purifying water containing 1,1,1-Trichloroethane", *Chem. Eng. Technol.*, **37**(3), 543-550.
Ghadiri, M., Fakhri, S. and Shirazian, S. (2014b), "Modeling of water transport through nanopores of membranes in direct-contact membrane distillation process", *Poly. Eng. Sci.*, **54**(3), 660-666.
Ghadiri, M., Parvini, M. and Darehnaei, M.G. (2014c), "Simulation of zinc extraction from aqueous solutions using polymeric hollow-fibers", *Poly. Eng. Sci.*, **54**(10), 2222-2227.
Ghadiri, M., Asadollahzadeh, M. and Hemmati, A. (2015), "CFD simulation for separation of ion from wastewater in a membrane contactor", *J. Water Process Eng.*, **6**, 144-150.
Hemmati, M., Nazari, N., Hemmati, A. and Shirazian, S. (2015), "Phenol removal from wastewater by means of nanoporous membrane contactors", *J. Ind. Eng. Chem.*, **21**, 1410-1416.
Huang, S.-M. and Yang, M. (2014), "Heat and mass transfer enhancement in a cross-flow elliptical hollow fiber membrane contactor used for liquid desiccant air dehumidification", *J. Membr. Sci.*, **449**, 184-192.
Huang, S.-M., Yang, M., Yang, Y. and Yang, X. (2013), "Fluid flow and heat transfer across an elliptical hollow fiber membrane tube bank for air humidification", *Int. J. Therm. Sci.*, **73**, 28-37.
Kneifel, K., Nowak W.A., Hilke, R., Just, R. and Peinemann, K.V. (2006), "Hollow fiber membrane contactor for air humidity control: Modules and membranes", *J. Membr. Sci.*, **276**(1-2), 241-251.
Kong, I.M., Choi, J.W., Kim, S.I., Lee, E.S. and Kim, M.S. (2015), "Experimental study on the self-humidification effect in proton exchange membrane fuel cells containing double gas diffusion backing layer", *Appl. Energ.*, **145**, 345-353.
Li, J. and Ito, A. (2008), "Dehumidification and humidification of air by surface-soaked liquid membrane module with triethylene glycol", *J. Membr. Sci.*, **325**(2), 1007-1012.
Miramini, S.A., Razavi, S.M.R., Ghadiri, M., Mahdavi, S.Z. and Moradi, S. (2013), "CFD simulation of acetone separation from an aqueous solution using supercritical fluid in a hollow-fiber membrane contactor", *Chem. Eng. Proces.: Process Intensifi.*, **72**, 130-136.
Moradi, S., Rajabi, Z., Mahammadi, M., Salimi, M., Homami, S.S., Seydei, M.K. and Shirazian, S. (2013), "3 dimensional hydrodynamic analysis of concentric draft tube airlift reactors with different tube diameters", *Math. Comput. Model.*, **57**(5-6), 1184-1189.
Nosratinia, F., Ghadiri, M. and Ghahremani, H. (2014), "Mathematical modeling and numerical simulation of ammonia removal from wastewaters using membrane contactors", *J. Ind. Eng. Chem.*, **20**(5), 2958-2963.
Paul, S.S., Ormiston, S.J. and Tachie, M.F. (2008), "Experimental and numerical investigation of turbulent cross-flow in a staggered tube bundle", *Int. J. Heat Fluid Flow*, **29**(2), 387-414.
Razavi, S.M.R., Razavi, S.M.J., Miri, T. and Shirazian, S. (2013), "CFD simulation of CO_2 capture from gas mixtures in nanoporous membranes by solution of 2-amino-2-methyl-1-propanol and piperazine", *Int. J. Greenhouse Gas Control*, **15**, 142-149.

Rezakazemi, M., Ghafarinazari, A., Shirazian, S. and Khoshsima, A. (2013a), "Numerical modeling and optimization of wastewater treatment using porous polymeric membranes", *Poly. Eng. Sci.*, **53**(6), 1272-1278.

Rezakazemi, M., Iravaninia, M., Shirazian, S. and Mohammadi, T. (2013b), "Transient computational fluid dynamics modeling of pervaporation separation of aromatic/aliphatic hydrocarbon mixtures using polymer composite membrane", *Poly. Eng. Sci.*, **53**(7), 1494-1501.

Roostaiy Ghalehnooiy, M., Marjani, A. and Ghadiri, M. (2015), "Synthesis and characterization of polyurethane/poly(vinylpyridine) composite membranes for desulfurization of gasoline", *RSC Advances*, **5**(116), 95994-96001.

Shirazian, S. and Ashrafizadeh, S.N. (2010), "Mass transfer simulation of caffeine extraction by subcritical CO_2 in a hollow-fiber membrane contactor", *Solvent Extr. Ion Exc.*, **28**(2), 267-286.

Shirazian, S. and Ashrafizadeh, S.N. (2011), "Near-critical extraction of the fermentation products by membrane contactors: A mass transfer simulation", *Ind. Eng. Chem. Res.*, **50**(4), 2245-2253.

Shirazian, S. and Ashrafizadeh, S.N. (2013), "3D modeling and simulation of mass transfer in vapor transport through porous membranes", *Chem. Eng. Technol.*, **36**(1), 177-185.

Shirazian, S., Marjani, A. and Rezakazemi, M. (2012a), "Separation of CO_2 by single and mixed aqueous amine solvents in membrane contactors: fluid flow and mass transfer modeling", *Eng. Comput.*, **28**(2), 189-198.

Shirazian, S., Pishnamazi, M., Rezakazemi, M., Nouri, A, Jafari, M. and Noroozi, S. (2012b), "Implementation of the finite element method for simulation of mass transfer in membrane contactors", *Chem. Eng. Technol.*, **35**(6), 1077-1084.

Tahvildari, K., Zarabpour, A., Ghadiri, M. and Hemmati, A. (2014), "Numerical simulation studies on heat and mass transfer using vacuum membrane distillation", *Poly. Eng. Sci.*, **54**(11), 2553-2559.

Wu, Y., Peng, X., Liu, J., Kong, Q., Shi, B. and Tong, M. (2002), "Study on the integrated membrane processes of dehumidification of compressed air and vapor permeation processes", *J. Membr. Sci.*, **196**(2), 179-183.

Zhang, L.-Z. (2012), "Coupled heat and mass transfer in an application-scale cross-flow hollow fiber membrane module for air humidification", *Int. J. Heat Mass Trans.*, **55**(21-22), 5861-5869.

Zhang, L.-Z. and Huang, S.-M. (2011), "Coupled heat and mass transfer in a counter flow hollow fiber membrane module for air humidification", *Int. J. Heat Mass Trans.*, **54**(5-6), 1055-1063.

Zhang, L.-Z. and Li, Z.-X. (2013), "Convective mass transfer and pressure drop correlations for cross-flow structured hollow fiber membrane bundles under low Reynolds numbers but with turbulent flow behaviors", *J. Membr. Sci.*, **434**, 65-73.

CC

Nomenclature

C	Concentration (mol/m^3)
$C_{H2O,m}$	Water concentration in the membrane side (mol/m^3)
$C_{H2O,s}$	Water concentration in the shell side (mol/m^3)
$C_{H2O,inlet}$	Water concentration in the inlet of shell side (mol/m^3)
$C_{H2O,inlet}$	Water concentration in the outlet of shell side (mol/m^3)
D	Diffusivity (m^2/s)
$D_{H2O,s}$	Moisture diffusivity in air (m^2/s)
$D_{H2O,m}$	Effective moisture diffusivity in membrane (m^2/s)
F	Body force (N)
K	Turbulence kinetic energy (m^2/s)
L	Effective fiber length (m)
N	Number of fiber
P	Pressure (pa)
R_i	Overall reaction rate of any species, mol/m^3·s
T	Temperature (K)
U	Velocity (m/s)
$U\infty$	Inlet velocity (m/s)
$U_{H2O,s}$	Velocity in the shell side (m/s)

Greek letters

ε	Energy dissipation rate (m^2/s^2/s), porosity
μ	Dynamic viscosity (pa·s)
ρ	Density (kg/m^3)
δ	Thickness of membrane (m)
η	Viscosity (kg/m·s)
σ_k	Effective Schmidt number for transport of K
σ_ε	Effective Schmidt number for transport of ε

Subscripts

T	Turbulent

Superscript

T	Turbulent
Sat	Saturation

Abbreviations

CFD	Computational fluid dynamics
FEM	Finite element method
HFMC	Hollow fiber membrane contactor
RH	Relative humidity
PVDF	Polyvinylidene fluoride